

1 Development of a coupled current-wave model
2 to assess the impact of a hurricane on particle
3 transport

4 Thomas Dobbelaere, Emmanuel Hanert

5 February 9, 2021

6 **Abstract**

7 In most hydrodynamic model studies, currents and waves are simu-
8 lated separately. This is especially true for the simulation of passive
9 drifters, whose trajectories are often computed based solely on cur-
10 rents. Although this simplification holds for most situations, as the
11 force exerted by waves on currents can be neglected in fair weather
12 conditions, it may lead to significant errors in storm conditions, during
13 which local currents are strongly influenced by wind-generated waves.
14 In this study, current-wave interactions in heavy-wind conditions are
15 studied by coupling the unstructured-mesh hydrodynamic model SLIM
16 with the wave model SWAN in the Florida Reef Tract during Hurricane
17 Irma (Sep. 2017). This coupled model successfully reproduced both
18 the observed wave behavior and storm surge during the hurricane.
19 The modeled currents were then used to simulate the trajectories of
20 passive drifters during the passage of the hurricane. Our results show
21 that taking wave force into account induces variations of up 1 m/s
22 in modelled currents on the continental shelf break as well as in the
23 vicinity of reefs and islands. Wave-current interactions can therefore
24 strongly modify the transport of drifting material, such as sediments
25 and coral larvae, during heavy-wind events. That should in particular
26 affect connectivity modeling studies since coral mass spawning events
27 tend to occur during the hurricane season in the Caribbean.

²⁸ **1 Introduction**

²⁹ **2 Methods**

³⁰ **2.1 Wind and atmospheric pressure for Hurricane Irma**

- ³¹ • Reduction of wind speed according to Harper et al. (2010)
- ³² • HURDAT 2 (Landsea and Franklin, 2013) for hurricane pressure with
³³ radius of maximum wind speed according to Knaff et al. (2018) using
³⁴ Holland pressure profile (Lin and Chavas, 2012).

³⁵ **2.2 Hydrodynamic model**

Ocean currents generated during hurricane Irma in the Florida Reef Tract (FRT) were modelled using the unstructured-mesh depth-integrated coast ocean model SLIM¹. The model mesh covers an area similar to the model extent of Dobbelaere et al. (2020), that includes the FRT but also the Florida Strait and part of the Gulf of Mexico (Figure 1). However, this area has been slightly extended northeastward and westward in order to include the location of buoys for wave outputs validation. Furthermore, in order to withstand potential cell drying due to storm conditions in this study, we used the conservative mode of SLIM with wetting-drying, whose equations write:

$$\begin{aligned} \frac{\partial H}{\partial t} + \nabla \cdot (\mathbf{U}) &= 0 \\ \frac{\partial \mathbf{U}}{\partial t} + \nabla \cdot \left(\frac{\mathbf{U}\mathbf{U}}{H} \right) &= -f\mathbf{e}_z \times \mathbf{U} + \alpha g H \nabla(H - h) - \frac{1}{\rho} \nabla p_{\text{atm}} + \frac{1}{\rho} \boldsymbol{\tau}_s \quad (1) \\ &\quad + \nabla \cdot (\nu \nabla \mathbf{U}) - \frac{C_b}{H^2} |\mathbf{U}| \mathbf{U} + \gamma(\mathbf{U}_* - \mathbf{U}) \end{aligned}$$

³⁶ where H is the water column height and \mathbf{U} is the depth-averaged transport;
³⁷ f is the Coriolis coefficient; g is the gravitational acceleration; h is the
³⁸ bathymetry; α is a coefficient stating whether the mesh element is wet
³⁹ ($\alpha = 1$) or dry ($\alpha = 0$); ν is the viscosity; C_b is the bottom drag coefficient;
⁴⁰ ∇p_{atm} is the atmospheric pressure gradient; $\boldsymbol{\tau}_s$ is the surface stress due to
⁴¹ wind; and γ is a relaxation coefficient towards a reference transport \mathbf{U}_* . As in

¹<https://www.slim-ocean.be>

42 Frys et al. (2020) and Dobbelaere et al. (2020), SLIM currents were relaxed
43 towards HYCOM (Chassignet et al., 2007) in regions where the water depth
44 exceeds a given threshold. At very high wind speeds, the white cap is blown
45 off the crest of the waves, which generates a layer of droplets that acts as
46 a slip layer for the winds at the ocean-atmosphere interface (Holthuijsen
47 et al., 2012). This causes a saturation of the wind drag coefficient for strong
48 winds (Donelan et al., 2004; Powell et al., 2003). To account for the impact
49 of this saturation on the surface wind stress in our model, we implemented
50 the wind drag parameterization of Moon et al. (2007).

51 The mesh resolution depended only on the distance to coastlines and reefs,
52 bathymetry and bathymetry gradient in order to satisfy SWAN refinement
53 criterion $h/A \geq a$, where h is the water depth and A is the element area. The
54 mesh was generated using the Python library seamsh², based on the the
55 open-source mesh generator GMSH (Geuzaine and Remacle, 2009) and is
56 composed of approximately 7.7×10^5 elements. The coarsest elements, far
57 away from the FRT, had a characteristic length size of about 5 km. Figure 1
58 depicts how a 100-m spatial resolution mesh simulated fine-scale details of
59 the ocean currents and significant wave height generated by hurricane Irma
60 in the Florida Keys.

61 **2.3 Wave model**

Waves were modelled using parallel unstructured SWAN (Booij et al., 1999)
on the same mesh as SLIM. This model solves the action balance equation,
which reads (Mei, 1989):

$$\frac{\partial N}{\partial t} + \nabla_{\mathbf{x}} \cdot [(\mathbf{c}_g + \mathbf{u})N] + \frac{\partial}{\partial \theta}[c_\theta N] + \frac{\partial}{\partial \sigma}[c_\sigma N] = \frac{S_{in} + S_{ds} + S_{nl}}{\sigma} \quad (2)$$

62 where N is the wave action density; θ is the wave propagation direction;
63 σ is the wave relative frequency; \mathbf{c}_g is the wave group velocity, \mathbf{u} is SLIM
64 depth-averaged current velocity; c_θ and c_σ are the propagation velocities in
65 spectral space due to refraction and shifting in frequency due to variations
66 in depth and currents; and S_{in} , S_{ds} , and S_{nl} respectively represent wave
67 growth by wind, wave decay and nonlinear transfers of wave energy through
68 interactions between triplets and quadruplets. Spectra were discretized with

²<https://pypi.org/project/seamsh/>

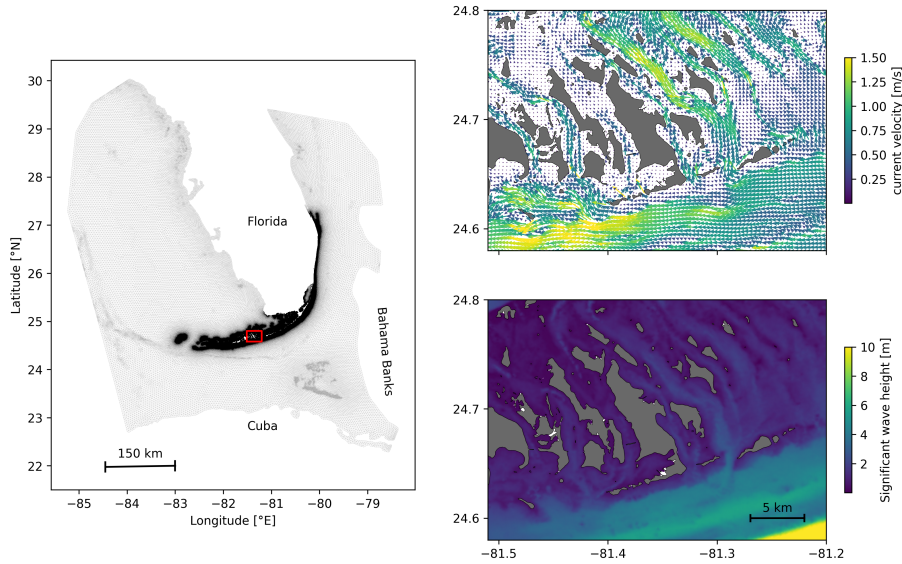


Fig. 1: Mesh of the computational domain with snapshots of simulated instantaneous currents and significant wave height on 2017-09-10 at 11:00:00. The mesh resolution ranges from 100 m in the Florida Keys to a maximum of 5 km offshore.

69 48 direction bins and 50 frequency bins logarithmically distributed from 0.3
 70 to 2 Hz. Exponential wind growth was parameterized using the formulation
 71 of Janssen (1991), while dissipations by whitecapping and bottom dissipa-
 72 tions followed the formulations of Komen et al. (1984) and Madsen et al.
 73 (1989) respectively. Coefficients for exponential wind growth and whitecap-
 74 ping parameterizations were based on the results of Siadatmousavi et al.
 75 (2011). Finally, wave boundary conditions were derived from WAVEWATCH
 76 III (Tolman et al., 2009) spectral outputs at buoy locations.

77 2.4 Coupled model

78 Express z_0 for Madsen bottom friction from Manning dissipation used in
 79 SLIM obtained following the methodology of Dietrich et al. (2011)

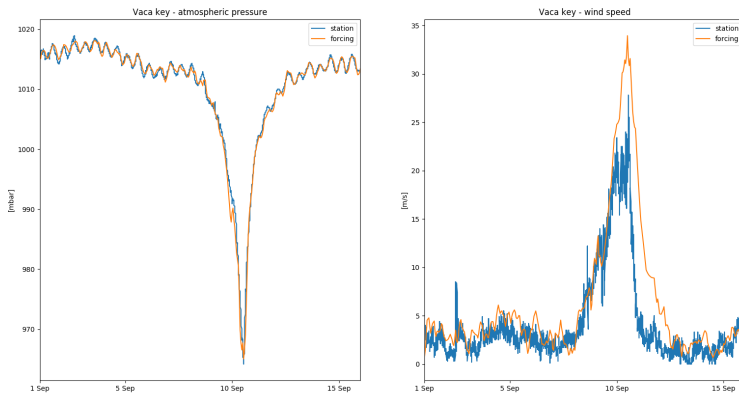


Fig. 2: The atmospheric forcings have been validated with meteorological station observations at Vaca Key. The reconstructed atmospheric pressure and wind speed agree well with field measurements.

80 3 Results

81 3.1 Validation

82 3.2 Impact of waves

83 4 Discussion and conclusions

84 Impact of waves on coral connectivity

85 Ability of wave model to correctly capture gradient in significant wave height
86 due to current-waves interactions under tropical cyclones depends on:

- 87 • Spatial (10km → 5km) and spectral (36 dir. → 48 dir.) resolution
88 (Hegermiller et al., 2019)
- 89 • Directional spreading of incident waves (Villas Bôas et al., 2020)

90 Conflict of Interest Statement

91 The authors declare that the research was conducted in the absence of any
92 commercial or financial relationships that could be construed as a potential

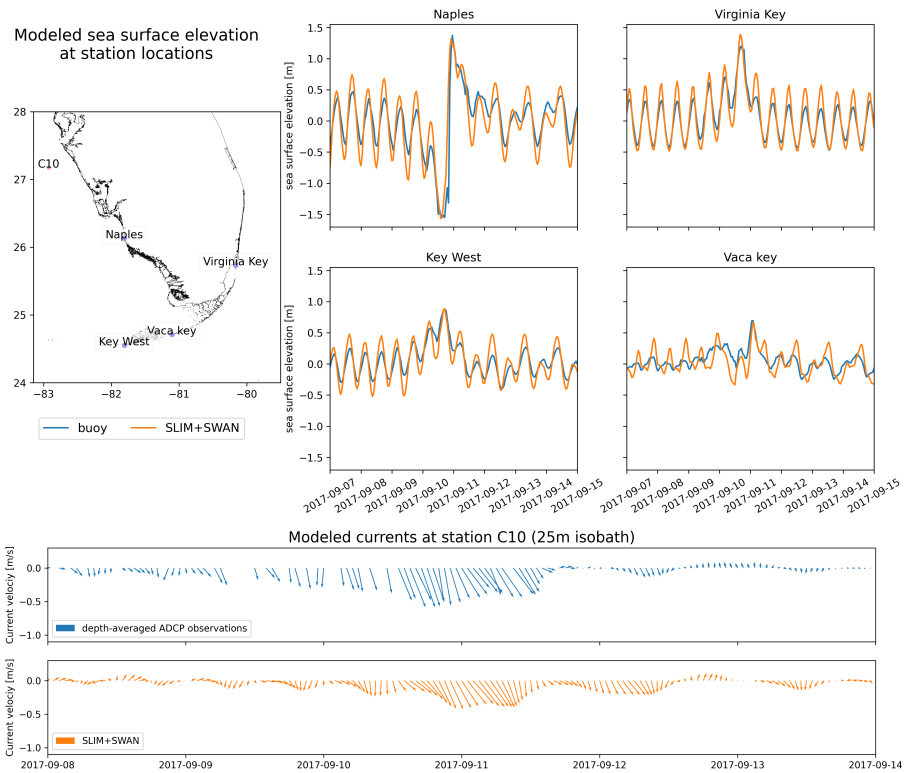


Fig. 3: The sea-surface elevation produced by the coupled wave-current model agrees with SSE and current velocity observations at different stations. The fit is particularly good in the Florida Keys and in Naples, on the inner Florida shelf. The coupled model currents have been validated against current meter data on the inner Florida shelf. The current speed and direction during the hurricane agrees well with the observations.

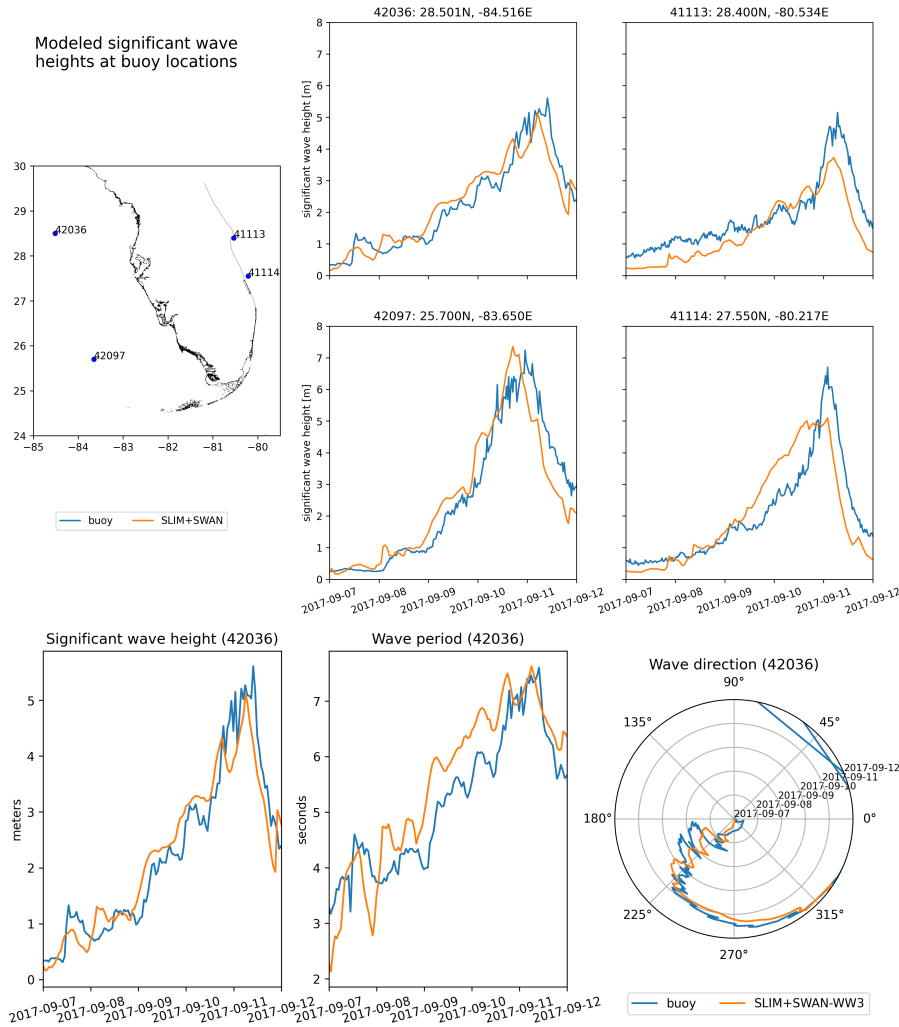


Fig. 4: The significant wave height produced by the coupled model has been compared to buoy measurements at 4 different stations. The timing and amplitude of the peak during the hurricane is correctly reproduced for all stations. For station 42036, the period and direction of the waves also agree well with observations

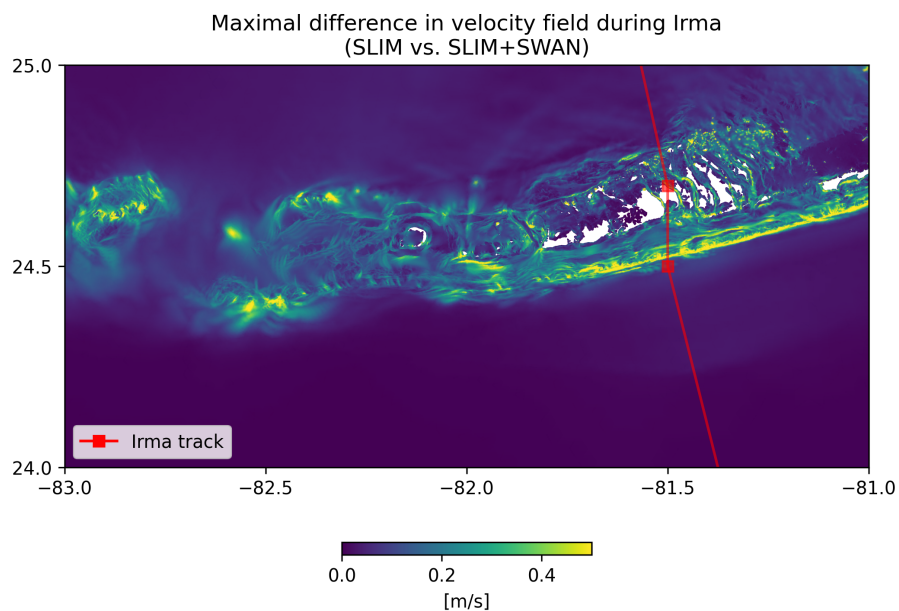


Fig. 5: Maximum of the difference between SLIM and SLIM+SWAN currents speed between 2017-09-07 00:00:00 and 2017-09-13 00:00:00. The difference between the coupled and uncoupled model, which represents the effect of the wave-induced stress, can yield differences of 0.5 m/s in the simulated currents during the passage of the hurricane. SLIM+SWAN currents velocities are larger than the currents modeled by SLIM alone.

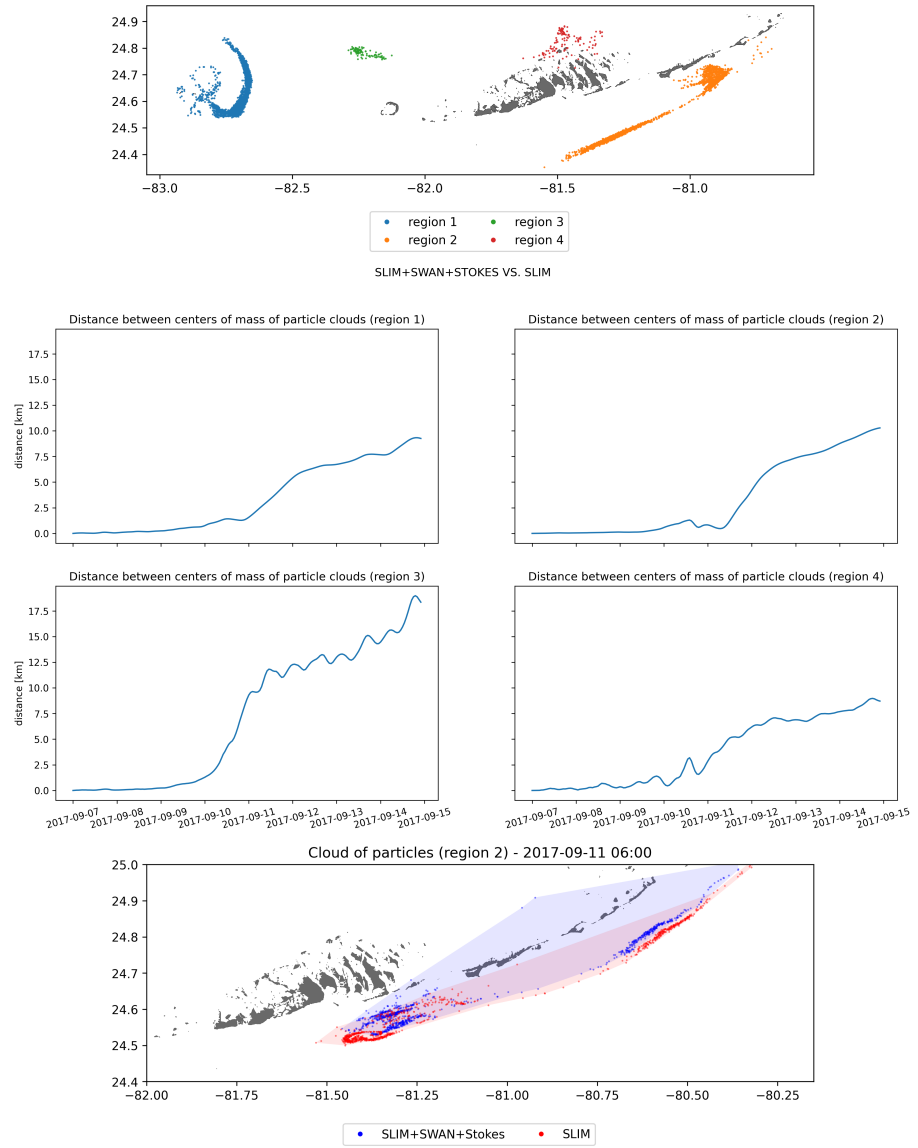


Fig. 6: Comparison of passive drifters trajectories with SLIM+SWAN+Stokes drift vs. SLIM alone. A snapshot of the positions of the particles released from region 2 is shown after the passage of Irma in the Florida Keys. Particles advected by the currents of the coupled model tend to remain on the shelf while particles advected by SLIM alone are mostly transported along the shelf break

⁹³ conflict of interest.

⁹⁴ **Author Contributions**

⁹⁵ **Funding**

⁹⁶ **Acknowledgments**

⁹⁷ Computational resources were provided by the Consortium des Équipements
⁹⁸ de Calcul Intensif (CÉCI), funded by the F.R.S.-FNRS under Grant No. 2.5020.11.
⁹⁹ Thomas Dobbelaere is a PhD student supported by the Fund for Research
¹⁰⁰ training in Industry and Agriculture (FRIA/FNRS).

¹⁰¹ **Supplementary Material**

¹⁰² The Supplementary Material for this article is attached to the submitted
¹⁰³ document.

¹⁰⁴ **References**

- ¹⁰⁵ Booij, N., Ris, R. C., and Holthuijsen, L. H. (1999). A third-generation wave
¹⁰⁶ model for coastal regions: 1. Model description and validation. *Journal*
¹⁰⁷ *of geophysical research: Oceans*, 104(C4):7649–7666.
- ¹⁰⁸ Chassignet, E. P., Hurlbert, H. E., Smedstad, O. M., Halliwell, G. R., Hogan,
¹⁰⁹ P. J., Wallcraft, A. J., Baraille, R., and Bleck, R. (2007). The HYCOM
¹¹⁰ (hybrid coordinate ocean model) data assimilative system. *Journal of*
¹¹¹ *Marine Systems*, 65(1-4):60–83.
- ¹¹² Dietrich, J., Westerink, J., Kennedy, A., Smith, J., Jensen, R., Zijlema, M.,
¹¹³ Holthuijsen, L., Dawson, C., Luettich, R., Powell, M., et al. (2011).
¹¹⁴ Hurricane gustav (2008) waves and storm surge: Hindcast, synoptic
¹¹⁵ analysis, and validation in southern Louisiana. *Monthly Weather Review*,
¹¹⁶ 139(8):2488–2522.

- 117 Dobbelaere, T., Muller, E. M., Gramer, L. J., Holstein, D. M., and Hanert, E.
118 (2020). Coupled epidemic-hydrodynamic modeling to understand the
119 spread of a deadly coral disease in Florida. *Frontiers in Marine Science*,
120 7:1016.
- 121 Donelan, M., Haus, B., Reul, N., Plant, W., Stiassnie, M., Gruber, H., Brown,
122 O., and Saltzman, E. (2004). On the limiting aerodynamic roughness of
123 the ocean in very strong winds. *Geophysical Research Letters*, 31(18).
- 124 Frys, C., Saint-Amand, A., Le Hénaff, M., Figueiredo, J., Kuba, A., Walker, B.,
125 Lambrechts, J., Vallaeyns, V., Vincent, D., and Hanert, E. (2020). Fine-
126 scale coral connectivity pathways in the Florida Reef Tract: implications
127 for conservation and restoration. *Frontiers in Marine Science*, 7:312.
- 128 Geuzaine, C. and Remacle, J.-F. (2009). Gmsh: A 3-d finite element mesh
129 generator with built-in pre-and post-processing facilities. *International
130 journal for numerical methods in engineering*, 79(11):1309–1331.
- 131 Harper, B., Kepert, J., and Ginger, J. (2010). *Guidelines for converting
132 between various wind averaging periods in tropical cyclone conditions*.
133 Citeseer.
- 134 Hegermiller, C. A., Warner, J. C., Olabarrieta, M., and Sherwood, C. R.
135 (2019). Wave-current interaction between Hurricane Matthew wave
136 fields and the Gulf Stream. *Journal of Physical Oceanography*,
137 49(11):2883–2900.
- 138 Holthuijsen, L. H., Powell, M. D., and Pietrzak, J. D. (2012). Wind and waves
139 in extreme hurricanes. *Journal of Geophysical Research: Oceans*,
140 117(C9).
- 141 Janssen, P. A. (1991). Quasi-linear theory of wind-wave generation applied
142 to wave forecasting. *Journal of physical oceanography*, 21(11):1631–
143 1642.
- 144 Knaff, J. A., Sampson, C. R., and Musgrave, K. D. (2018). Statistical tropi-
145 cal cyclone wind radii prediction using climatology and persistence:
146 Updates for the western North Pacific. *Weather and Forecasting*,
147 33(4):1093–1098.

- 148 Komen, G., Hasselmann, S., and Hasselmann, K. (1984). On the exis-
149 tence of a fully developed wind-sea spectrum. *Journal of physical*
150 *oceanography*, 14(8):1271–1285.
- 151 Landsea, C. W. and Franklin, J. L. (2013). Atlantic hurricane database un-
152 certainty and presentation of a new database format. *Monthly Weather*
153 *Review*, 141(10):3576–3592.
- 154 Lin, N. and Chavas, D. (2012). On hurricane parametric wind and appli-
155 cations in storm surge modeling. *Journal of Geophysical Research: Atmospheres*, 117(D9).
- 157 Madsen, O. S., Poon, Y.-K., and Gruber, H. C. (1989). Spectral wave
158 attenuation by bottom friction: Theory. In *Coastal Engineering 1988*,
159 pages 492–504.
- 160 Mei, C. C. (1989). *The applied dynamics of ocean surface waves*, volume 1.
161 World scientific.
- 162 Moon, I.-J., Ginis, I., Hara, T., and Thomas, B. (2007). A physics-based
163 parameterization of air–sea momentum flux at high wind speeds and
164 its impact on hurricane intensity predictions. *Monthly weather review*,
165 135(8):2869–2878.
- 166 Powell, M. D., Vickery, P. J., and Reinhold, T. A. (2003). Reduced drag coeffi-
167 cient for high wind speeds in tropical cyclones. *Nature*, 422(6929):279–
168 283.
- 169 Siadatmousavi, S. M., Jose, F., and Stone, G. (2011). Evaluation of two WAM
170 white capping parameterizations using parallel unstructured SWAN
171 with application to the Northern Gulf of Mexico, USA. *Applied Ocean*
172 *Research*, 33(1):23–30.
- 173 Tolman, H. L. et al. (2009). User manual and system documentation of
174 WAVEWATCH III TM version 3.14. *Technical note, MMAB Contribution*,
175 276:220.
- 176 Villas Bôas, A. B., Cornuelle, B. D., Mazloff, M. R., Gille, S. T., and Arduin,
177 F. (2020). Wave–current interactions at meso-and submesoscales:
178 Insights from idealized numerical simulations. *Journal of Physical*
179 *Oceanography*, 50(12):3483–3500.